

## OPEN ACCESS

EDITED BY  
Charbel Moussa,  
Georgetown University, United States

REVIEWED BY  
Luke William Bonham,  
University of California, San Francisco,  
United States  
Oliver Bracko,  
University of Miami, United States

\*CORRESPONDENCE  
Carolyn A. Fredericks  
✉ carolyn.fredericks@yale.edu

SPECIALTY SECTION  
This article was submitted to  
Translational Research in Dementia,  
a section of the journal  
Frontiers in Dementia

RECEIVED 16 December 2022  
ACCEPTED 28 February 2023  
PUBLISHED 20 March 2023

CITATION  
Ju S, Horien C, Shen X, Abuwarda H, Trainer A,  
Constable RT and Fredericks CA (2023)  
Connectome-based predictive modeling  
shows sex differences in brain-based predictors  
of memory performance.  
*Front. Dement.* 2:1126016.  
doi: 10.3389/frdem.2023.1126016

COPYRIGHT  
© 2023 Ju, Horien, Shen, Abuwarda, Trainer,  
Constable and Fredericks. This is an  
open-access article distributed under the terms  
of the [Creative Commons Attribution License  
\(CC BY\)](https://creativecommons.org/licenses/by/4.0/). The use, distribution or reproduction  
in other forums is permitted, provided the  
original author(s) and the copyright owner(s)  
are credited and that the original publication in  
this journal is cited, in accordance with  
accepted academic practice. No use,  
distribution or reproduction is permitted which  
does not comply with these terms.

# Connectome-based predictive modeling shows sex differences in brain-based predictors of memory performance

Suyeon Ju<sup>1</sup>, Corey Horien<sup>2</sup>, Xilin Shen<sup>3</sup>, Hamid Abuwarda<sup>1</sup>,  
Anne Trainer<sup>1</sup>, R. Todd Constable<sup>3</sup> and Carolyn A. Fredericks<sup>1\*</sup>

<sup>1</sup>Department of Neurology, Yale School of Medicine, New Haven, CT, United States, <sup>2</sup>Interdepartmental Neuroscience Program, Yale School of Medicine, New Haven, CT, United States, <sup>3</sup>Department of Radiology and Biomedical Imaging, Yale School of Medicine, New Haven, CT, United States

Alzheimer's disease (AD) takes a more aggressive course in women than men, with higher prevalence and faster progression. Amnesic AD specifically targets the default mode network (DMN), which subserves short-term memory; past research shows relative hyperconnectivity in the posterior DMN in aging women. Higher reliance on this network during memory tasks may contribute to women's elevated AD risk. Here, we applied connectome-based predictive modeling (CPM), a robust linear machine-learning approach, to the Lifespan Human Connectome Project-Aging (HCP-A) dataset ( $n = 579$ ). We sought to characterize sex-based predictors of memory performance in aging, with particular attention to the DMN. Models were evaluated using cross-validation both across the whole group and for each sex separately. Whole-group models predicted short-term memory performance with accuracies ranging from  $\rho = 0.21$ – $0.45$ . The best-performing models were derived from an associative memory task-based scan. Sex-specific models revealed significant differences in connectome-based predictors for men and women. DMN activity contributed more to predicted memory scores in women, while within- and between- visual network activity contributed more to predicted memory scores in men. While men showed more segregation of visual networks, women showed more segregation of the DMN. We demonstrate that women and men recruit different circuitry when performing memory tasks, with women relying more on intra-DMN activity and men relying more on visual circuitry. These findings are consistent with the hypothesis that women draw more heavily upon the DMN for recollective memory, potentially contributing to women's elevated risk of AD.

## KEYWORDS

healthy aging, default mode network, sex differences, functional MRI, connectome-based predictive modeling

## 1. Introduction

In addition to outnumbering men with Alzheimer's disease (AD) by 2:1 ('2022 Alzheimer's disease facts figures', 2022), women with AD face faster accumulation of pathology and more severe illness with the same pathologic burden (Barnes et al., 2005; Buckley et al., 2018; Edwards et al., 2021). AD specifically targets the default mode network (DMN), which subserves short-term memory (Greicius et al., 2004; Sheline et al., 2010; Mormino et al., 2011; Brier et al., 2012). Yet,

sex differences in the DMN over the course of aging, which may provide important clues to women's higher vulnerability to AD, are poorly understood.

Prior research assessing sex differences in the aging brain has demonstrated that healthy aging women show lower segregation of functional networks (i.e., more cross-hemispheric/module connections; [Ingalhalikar et al., 2014](#)). Women have relatively higher DMN connectivity overall ([Biswal et al., 2010](#); [Ferretti et al., 2018](#); [Ritchie et al., 2018](#)), and demonstrate higher connectivity than men in posterior DMN nodes, which relates to short-term memory performance ([Ficek-Tani et al., 2022](#)).

Prediction-based approaches, in which models are built on training data and tested on unseen data, can help increase generalizability and reproducibility of findings ([Yarkoni and Westfall, 2017](#); [Scheinost et al., 2019](#); [Poldrack et al., 2020](#); [Marek et al., 2022](#); [Yarkoni, 2022](#)), and have the potential to generate useful biomarkers ([Gabrieli et al., 2015](#); [Rosenberg et al., 2018](#)).

In this work, we use a predictive modeling-based approach to robustly characterize sex differences in the aging functional connectome. We used connectome-based predictive modeling (CPM) to predict short-term memory performance scores in a large dataset of healthy adults aged 36–100. We hypothesized that (a) predictive edges would vary substantially between men and women, (b) predictors would especially feature the DMN, with women relying more on within-DMN edges for memory task performance, and (c) women would show decreased network segregation than do men.

## 2. Methods

### 2.1. Participants

The data used were collected from participants enrolled in the Human Connectome Project-Aging (HCP-A) study ([Bookheimer et al., 2019](#)). Neuropsychological data were drawn from the 2.0 release, which included updates to these data. Imaging data were from the 1.0 release of the HCP-A dataset, as raw imaging data was not updated for the 2.0 release. Imaging data consisted of 689 healthy subjects aged 36 to 100 from four data collection sites. See [Bookheimer et al. \(2019\)](#) for full exclusion criteria. As described previously ([Ficek-Tani et al., 2022](#)), we implemented additional exclusion criteria based on motion (see below for details), missing data, and anatomical abnormalities. After exclusion, the remaining sample size was  $n = 579$  (330 female; 249 male).

Participants were well-matched in age, race, ethnicity, years of education, and handedness, but women outnumbered and outperformed men in global cognitive function (Montreal Cognitive Assessment), in-scanner memory task performance (FaceName task), and verbal learning (Rey Auditory Verbal Learning Test; [Table 1](#)). Participants self-identified their sex at birth as male or female. While an "Other" option for sex was offered by the HCP-A study, no participants chose this option; gender identity was not assessed.

### 2.2. Imaging parameters

All subjects enrolled in HCP-A were scanned in a Siemens 3T Prisma scanner with 80 mT/m gradients and 32-channel head coil. In addition to acquiring four resting-state fMRI (rfMRI) and three task-fMRI (tfMRI) scans per subject, structural MRI data [including one T1-weighted (T1w) scan] were also collected ([Harms et al., 2018](#)). In this study, we focus on the seven fMRI scans.

A multi-echo MPRAGE sequence [refer to [Harms et al. \(2018\)](#) for scanning parameter details] was used for all T1w scans. A 2D multiband (MB) gradient-recalled echo (GRE) echo-planar imaging (EPI) sequence (MB8, TR/TE = 800/37 ms, flip angle = 52°) was used for all fMRI scans.

For each subject, four rfMRI scans consisting of 488 frames and lasting 6.5 min each (for a total of 26 min) were acquired, during which participants were instructed to remain awake while viewing a small white fixation cross in the center of a black background. The rfMRI scans were split between two sessions that occurred on the same day, with each session including one rfMRI with an anterior to posterior (AP) phase encoding direction and one rfMRI with a posterior to anterior (PA) direction.

The HCP-A includes the following three fMRI tasks, which were all programmed in PsychoPy ([Peirce, 2007, 2008](#)) and collected with PA phase encoding direction: Visuomotor (VisMotor), Conditioned Approach Response Inhibition Task ("CARIT" Go/NoGo task), and FaceName ([Bookheimer et al., 2019](#)). As below, we focus on the FaceName task scan both because of its relevance to short-term memory performance and because models derived from this scan outperform models derived from other scans. In the FaceName task, three blocks (encoding, distractor, and recall blocks) are repeated twice for each set of faces, totaling to a single, 276-second run. See [Harms et al. \(2018\)](#) for full details on the HCP-A structural and functional MRI imaging parameters, and see [Bookheimer et al. \(2019\)](#) for full details on tfMRI task administration.

### 2.3. Image preprocessing

The preprocessing approach has been described elsewhere ([Greene et al., 2018](#); [Horien et al., 2019](#)). MPRAGE scans were skullstripped with optiBET ([Lutkenhoff et al., 2014](#)) and nonlinearly registered to the MNI template in BioImage Suite (BIS; [Joshi et al., 2011](#)). BIS was used to linearly register each participant's mean functional scan to their own MPRAGE scan. Skull-stripped and registered data were visually inspected for structural abnormalities and distortions, and participants were excluded for significant structural lesions including meningioma, vascular abnormalities or ventriculomegaly significant enough to distort cortical anatomy, as well as for significant scanner artifacts. Functional data were motion-corrected using SPM8; participants whose scans showed maximum mean frame-to-frame displacement (FFD) above 0.3 mm were excluded to limit motion artifacts ([Greene et al., 2018](#); [Horien et al., 2018, 2019](#); [Ju et al., 2020](#)). Using Wilcoxon rank sum tests, we determined no differences in mean FFD between female and male subjects across all seven scan

**TABLE 1** Demographics and selected neuropsychological assessment and in-scanner task scores of HCP-A participants included in this study (Costa and McCrae, 1992; Nasreddine et al., 2005; Bean, 2011; Bookheimer et al., 2019).

	Female subjects	Male subjects	P-value
Total number of participants	330 (57%)	249 (43%)	N/A
Age	56.94 (14.03)	58.20 (14.13)	0.284
Race	American Indian/Alaska Native: 1 Asian: 19 Black/African American: 53 White: 231 More than one race: 18 Unknown/Not reported: 8	American Indian/Alaska Native: 1 Asian: 26 Black/African American: 34 White: 177 More than one race: 9 Unknown/Not reported: 2	0.167
Ethnicity	Hispanic or Latino: 36 Not Hispanic or Latino: 293 Unknown/Not reported: 1	Hispanic or Latino: 18 Not Hispanic or Latino: 231 Unknown/Not reported: 0	0.216
Years of Education	15.38 (1.76)	15.62 (1.82)	0.121
Handedness	Right: 283 Left: 21 Ambidextrous: 26	Right: 197 Left: 21 Ambidextrous: 31	0.100
MOCA Total (points out of 30)	26.86 (2.24)	26.21 (2.56)	1.24E-3
FaceName Task Total (# face-name pairs recalled, out of 10)	6.97 (2.72)	5.90 (2.96)	1.27E-5
RAVLT Sum of Trials 1–5 (# words recalled, out of 75)	48.22 (9.71)	44.06 (10.50)	1.44E-6
RAVLT Trial 6 (# words recalled, out of 15)	10.13 (2.99)	9.07 (3.31)	7.47E-5

T-tests or chi square tests were performed as appropriate, excluding unknown/not reported values. MOCA, Montreal Cognitive Assessment; RAVLT, Rey Auditory Verbal Learning Test.

types (Supplementary Table 1). Linear, quadratic, and cubic drift, a 24-parameter model of motion (Satterthwaite et al., 2013), mean cerebrospinal fluid signal, mean white matter signal, and global signal were regressed from the data as described in Ficek-Tani et al. (2022).

## 2.4. Memory performance measures

Because we were interested in predictors of memory performance, we used performance on the FaceName task and the Rey Auditory Verbal Learning Test (RAVLT) as outcomes for our predictive models. For the FaceName task, participants were shown a total of 10 distinct faces, resulting in a maximum FaceName-Total Recall (FN-TR) score of 10 correctly identified faces. We also assessed both the learning (L) and immediate recall (IR) metrics from the RAVLT (Bean, 2011), a standard neuropsychological measure of declarative memory. In this assessment, a 15-word list is read to the participant, who is then asked to verbally recall as many as possible, five times. The total number of words recalled during this five-trial “learning period” sums to a RAVLT-L (“learning”) score out of 75 words. After being read a separate (interference) list and asked to recall it, the participant is read List A again, and the number of correctly-recalled words in this sixth trial is collected as the RAVLT-IR (“immediate recall”) score. RAVLT-IR is a sensitive metric for early-stage AD (Estévez-González et al., 2003).

## 2.5. Connectome-based predictive modeling

To predict memory performance using both rfMRI and tfMRI data from HCP-A, we used connectome-based predictive modeling (CPM), the details of which are described elsewhere (Shen et al., 2017).

In brief, connectivity matrices were constructed from each fMRI scan using the Shen 268-node atlas (Shen et al., 2013). These matrices and the memory performance scores of each participant were used to create our predictive models. Three subject groups were analyzed: all subjects, female-only, and male-only. Edges from connectivity matrices for each subject per scan were correlated to the three aforementioned memory performance measures, totaling to seven connectivity matrices and three memory scores per subject (21 total correlated matrices). Motion and age covariates were also included in the CPM analyses to account for in-scanner head motion, age, and their interaction in our predictions, as previously done (Scheinost et al., 2021; Dufford et al., 2022; Horien et al., 2022).

Using 5-fold cross validation, connectivity matrices and memory scores were divided into independent training (subjects from four of the folds) and testing (subjects in left-out fold) sets. Edge strength and memory were linearly related within the training set, and using a feature selection threshold of  $p = 0.01$ , a consensus connectivity matrix including only the edges most strongly positively or negatively correlated to memory was generated. Edge strengths in each subject’s connectivity matrix

corresponding to the consensus matrix were summed into a single-subject connectivity value. A predictive model built using the linear relationship between the single-subject connectivity values and memory score was applied to the subjects in the testing set to generate memory performance predictions.

## 2.6. Model performance comparison

For all subject groups, Spearman's correlation and root mean square error [defined as:  $RMSE(\text{predicted}, \text{observed}) = \sqrt{(1/n \sum_{i=1}^n (\text{actual}_i - \text{predicted}_i)^2)}$ ] were used to compare the similarity between predicted and observed memory scores to assess predictive model performance. After performing 1,000 iterations of each CPM analysis, we selected the median-performing model to represent the model's overall performance. To compare model performances between female and male groups for each fMRI scan, we used Wilcoxon rank sum tests.

We also tested our models against randomly permuted models by randomly shuffling participant labels prior to attempting to predict memory scores. After performing 1,000 iterations of this permutation, we calculated the number of times the permuted predictive accuracy was greater than the median unpermuted prediction accuracy to generate a non-parametric  $p$ -value, as done in Scheinost et al. (2021):

$$P = (\#\{rho_{null} \geq rho_{median}\})/1000,$$

where  $\#\{rho_{null} \geq rho_{median}\}$  indicates the number of permuted predictions numerically greater than or equal to the median of the unpermuted predictions. We applied the Benjamini-Hochberg procedure to these non-parametric  $p$ -values to control for multiple comparisons and correct for 21 tests for each of our three subject groups (Benjamini and Hochberg, 1995).

## 2.7. Inter-network significant-edge analyses

To visualize sex differences at the network level, we first split the aforementioned consensus matrix into two binarized matrices (a "positive" matrix containing edge with significant positive correlations to memory and the other "negative" matrix of edges with significant negative correlations to memory) for each predictive model. Categorization of nodes by functional network was determined using the 10-network parcellation of the Shen 268-node atlas (Horien et al., 2022). In this network grouping, the medial frontal (MF) network also includes some temporal and frontal nodes which often cluster with the DMN. Inter-network edges were defined as the number of significant edges between each pair of networks normalized by the total number of edges between the same network pair. As done in previous work, we defined edges as "significant" if they appear in at least 2 out of 5 folds in 40% of 1,000 iterations of CPM to minimize noise while retaining meaningful connections (Rosenberg et al., 2016; Yip et al., 2019; Horien et al., 2022). In addition to using heatmaps to visualize the inter-network edges of both female and male groups separately, we

subtracted male-group positive edges from female-group positive edges (and the same with the negative edges) across corresponding matrix cells to evaluate the inter-network sex differences. Following this, we used the same internally cross-validated procedure as above to apply our sex-based models on subjects of the opposite sex (i.e., testing male-data-trained models on female subject data, and vice versa) and see if they were adequate predictors for the other sex.

## 2.8. Intra-network significant-edge analyses

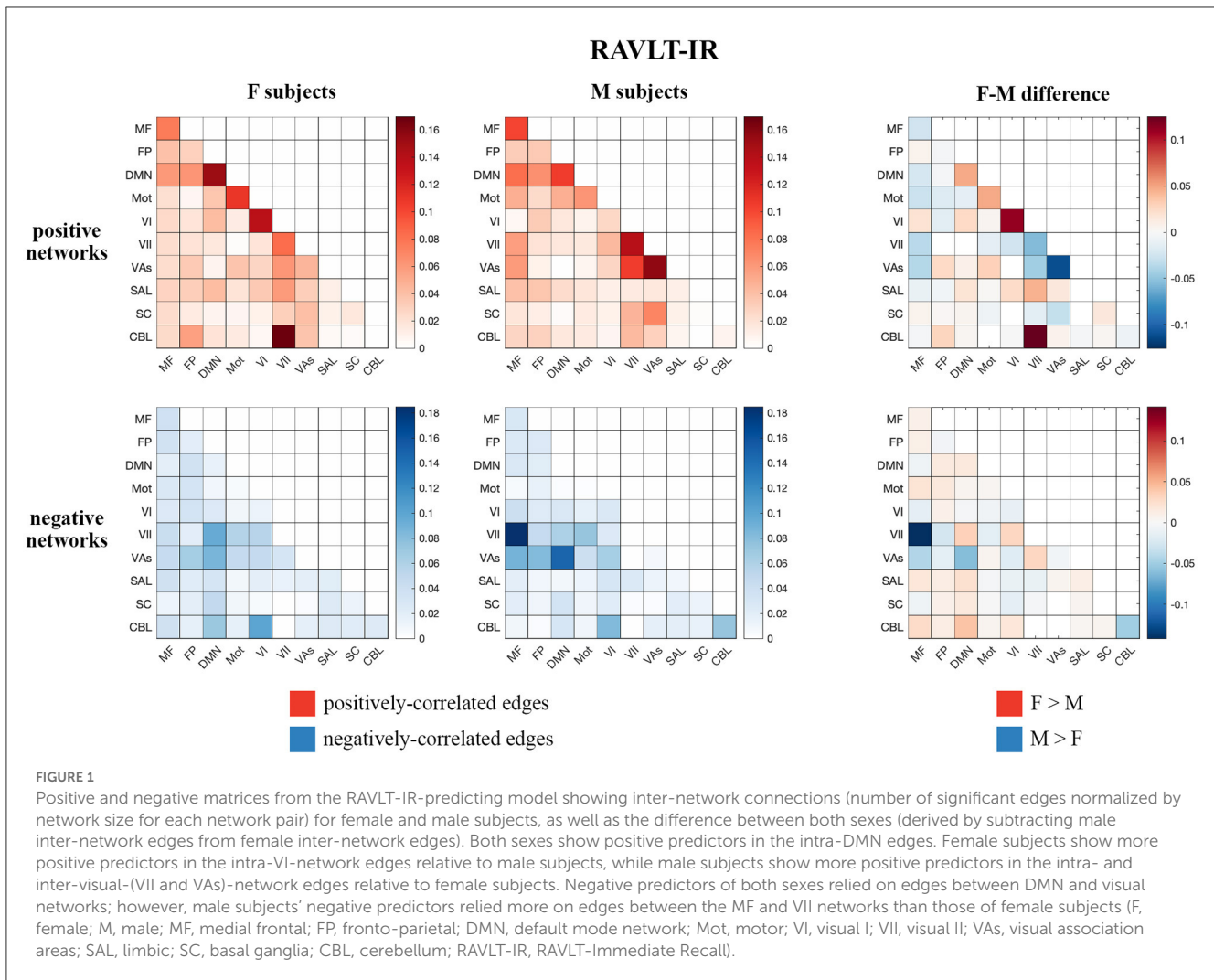
Intra-network analyses were performed similarly to inter-network analyses above. Edges from binarized positively and negatively correlated connectivity matrices were summed across the 5 folds and 1,000 iterations to generate a single value for each edge. These values were then used to generate the intra-DMN edge heatmap, with values ranging from  $-5,000$  (maximum negatively correlated) to  $5,000$  (maximum positively correlated value). To evaluate differences in the "top-performing" nodes according to sex, individual edge values were summed across each row from the matrices, and divided by 2 to account for the symmetric nature of the matrix, generating a summed vector (SV).

## 2.9. Network segregation analyses

We evaluated network segregation, a measure of the relative strength of within-network connections to between-network connections, using a novel association ratio metric. We defined the association ratio as the weighted sum of all edges within the network of interest, normalized by the weighted sum of all edges between this network and the whole set of regions of interest. Higher association ratio is therefore indicative of higher network segregation. To compare network segregation levels between sexes, we calculated and compared (using two-sample  $t$ -tests) the association ratio for certain networks of interest in women and men for each scan type. Benjamini-Hochberg correction (see above) was applied to correct for 7 significance tests (for each model) across the 4 networks.

## 2.10. Data and code availability

Data from the HCP-A study are openly available (<https://www.humanconnectome.org/study/hcp-lifespan-aging/data-releases>). Image preprocessing was performed using BioImageSuite, a publicly-available software (<https://medicine.yale.edu/bioimaging/suite/>). Scripts for running CPM are available through GitHub (<https://github.com/YaleMRRRC/CPM>). Other MATLAB scripts for CPM analyses can be found at [https://github.com/frederickslab/CPM\\_HCP-A\\_sex\\_difference\\_study](https://github.com/frederickslab/CPM_HCP-A_sex_difference_study). Custom MATLAB colormap palettes were derived from ColorBrewer (<http://colorbrewer.org/>; Brewer, 2022).



### 3. Results

#### 3.1. Model performance comparison

Please see [Supplementary Methods/Results](#) for details on model comparisons, including comparisons between models derived separately for each sex. Briefly, we trained and cross-validated models using functional connectivity data from all 7 scans to predict memory performance scores. Whole-group models robustly predicted all memory measures, with accuracies ranging from Spearman's  $\rho = 0.21$  ( $RMSE = 3.34, p < 0.0001$ ) to  $\rho = 0.45$  ( $RMSE = 2.67, p < 0.0001$ ) across all models ([Supplementary Figure 1](#)). Models using the FaceName tfMRI scan consistently outperformed all other models; we therefore proceeded with models from this scan for the remaining analyses.

#### 3.2. Inter-network significant-edge analyses

Visualizations of inter-network edges (number of significant edges normalized by network size) across all FaceName tfMRI

models revealed differences in key edges predicting memory score for each sex. In particular, edges within the DMN and visual (visual I [VI], visual II [VII], and visual association areas [VAs]) networks showed the largest differences ([Figure 1](#), [Supplementary Figure 5](#)). Given previous work showing measures of declarative verbal memory (including RAVLT metrics) can be predicted from the gray matter density of DMN structures, and because lower RAVLT-IR scores are associated with preclinical AD, we concentrated on the RAVLT-IR predictors derived from FaceName tfMRI models ([Estévez-González et al., 2003](#); [Moradi et al., 2017](#)). In addition to visualizing the inter-network edges of females and males separately, we subtracted male-group edges from female-group edges across corresponding heatmap cells to evaluate inter-network differences between the sexes ([Figure 1](#)).

Both sexes show positive predictors with intra-DMN edges, with female scores predicting intra-DMN connectivity more strongly than those of males. Female positive predictors also relied more strongly on intra-VI edges than those of males, while male positive predictors relied more strongly on the intra- and inter-network connectivity of the VII and VAs networks relative to those of females. Both sexes displayed negative predictors with edges between DMN and visual networks; however, males show

more negative predictors with edges between the MF and VII networks, as well as between the DMN and VII networks, relative to females. Additionally, testing our sex-based models on subjects of the opposite sex revealed that our female models successfully predicted outcomes for male subjects across all our memory tasks, while our male models successfully predicted only the RAVLT-L outcome for female subjects (see [Supplementary Table 10](#) for model performance statistics).

### 3.3. Intra-network significant-edge analyses

Given the preferential contribution of intra-DMN edges to the female models, we examined all intra-DMN edges and evaluated their strengths in male and female models. To do so, we generated a heatmap of intra-DMN edges ([Figure 2](#)). In the RAVLT-IR model, we found that edges from more posterior DMN nodes were preferentially increased in females as opposed to males. This trend held true for the RAVLT-L model and FN-TR models ([Supplementary Figure 7](#)). Negatively correlated edges negligibly contributed to both male and female models ([Figure 2](#), [Supplementary Figure 7](#)). Both sexes displayed strong connections in the left posterior cingulate cortex (L PCC) and precuneus, known hubs of the DMN.

To summarize node-level differences, we summed the number of edges associated with each node and found consistent female preference for activity of the right posterior inferior parietal lobe (R pIPL) and left anterior medial prefrontal cortex (L amPFC)/paracingulate cortex ([Figure 2](#)). The R pIPL was consistently and preferentially elevated in all female models analyzed ([Supplementary Figure 7](#)).

### 3.4. Network segregation analyses

We then evaluated and compared a metric of network segregation (see Methods, “Network Segregation Analysis”) within the DMN and visual (VI, VII, VAs) networks between females and males, given the strong brain-behavior correlations in these networks across all memory performance outcomes. Our analysis demonstrated increased network segregation of the DMN in females relative to males, and increased network segregation of VII and VAs in males relative to females ([Table 2](#)). Additionally, these findings echoed our previous CPM analysis results in that we also observed sex differences in neurobiological organization.

## 4. Discussion

We use CPM to identify sex differences in the functional connectivity underlying memory performance in a large sample of healthy aging adults. We provide evidence that distinct edges for men and women predict short-term verbal memory task performance, and that within-DMN edges contribute more to memory scores in females than in males. Predictive edges for males, in contrast, include more edges within and across visual

sensory and association networks. In contrast to prior literature suggesting globally decreased network segregation in older women compared with men, we also show higher segregation of the DMN (but lower segregation of visual sensory and association networks) in women.

These findings imply that when compared with males, females have a higher reliance upon connections within the DMN, the intrinsic connectivity network targeted in AD, in performing memory-related tasks. Increased DMN connectivity, particularly in posterior nodes, has been associated with vulnerability to Alzheimer’s disease ([Bookheimer et al., 2000](#); [Filippini et al., 2009](#); [Sperling et al., 2009](#); [Mormino et al., 2011](#); [Schultz et al., 2017](#)); increased connectivity in preclinical AD settings is thought to represent the compensatory response of a network under stress ([Bondi et al., 2005](#); [Filippini et al., 2009](#); [Qi et al., 2010](#); [Mormino et al., 2011](#)), and symptomatic disease is associated with progressive hypoconnectivity across the network ([Greicius et al., 2004](#); [Sheline et al., 2010](#); [Brier et al., 2012](#)).

This study and our previous findings in the same dataset ([Ficek-Tani et al., 2022](#)) converge on an emerging narrative of increased connectivity and functional segregation of the DMN in aging women. Women rely upon specific DMN edges for memory performance; connections between the bilateral pIPL and the two greatest hubs of the DMN, the mPFC and the PCC/precuneus are the strongest predictors. Our prior work suggests that women have relatively increased within-DMN connectivity compared with men, particularly in posterior nodes and particularly during perimenopausal decades ([Ficek-Tani et al., 2022](#)). Reliance upon intra-DMN edges for memory performance likely has its advantages: we and others have shown that DMN connectivity, particularly between posterior nodes, correlates with memory task performance ([Fredericks et al., 2019](#); [Natu et al., 2019](#); [Kang et al., 2021](#); [Vanneste et al., 2021](#); [Ficek-Tani et al., 2022](#)), and the literature consistently demonstrates that women outperform men across the lifespan in tests of verbal episodic memory ([Bleeker et al., 1988](#); [Herlitz et al., 1997](#); [Golchert et al., 2019](#)). We also noted that there were more positive than negative correlations for intra-DMN edges predicting memory performance in both women and men. We believe this finding reflects the strong and well-established positive relationship between connectivity within the DMN and short-term memory performance ([Greicius et al., 2004](#); [Sheline et al., 2010](#); [Mormino et al., 2011](#); [Brier et al., 2012](#)). When we tested our female models on male subjects, and vice versa, we discovered that they both performed well in predicting memory outcomes for subjects of the opposite sex ([Supplementary Table 10](#)). This suggests that while the models themselves may be complex, there may be a common “core” architecture that allows for predictive power across subgroups despite meaningful network connectivity differences between those subgroups.

We also find relatively greater functional segregation of the DMN in women than in men. Functional segregation (i.e., reliance on within- more than between-network connectivity to perform a network-associated task) declines across the brain with aging, and is associated with decreased performance on tests of attention and memory performance ([Chan et al., 2014](#); [Geerligs et al., 2015](#); [Ng et al., 2016](#)). AD pathology is associated with decreased functional segregation ([Cassady et al., 2021](#)), and prior work in this field has suggested that women show decreased

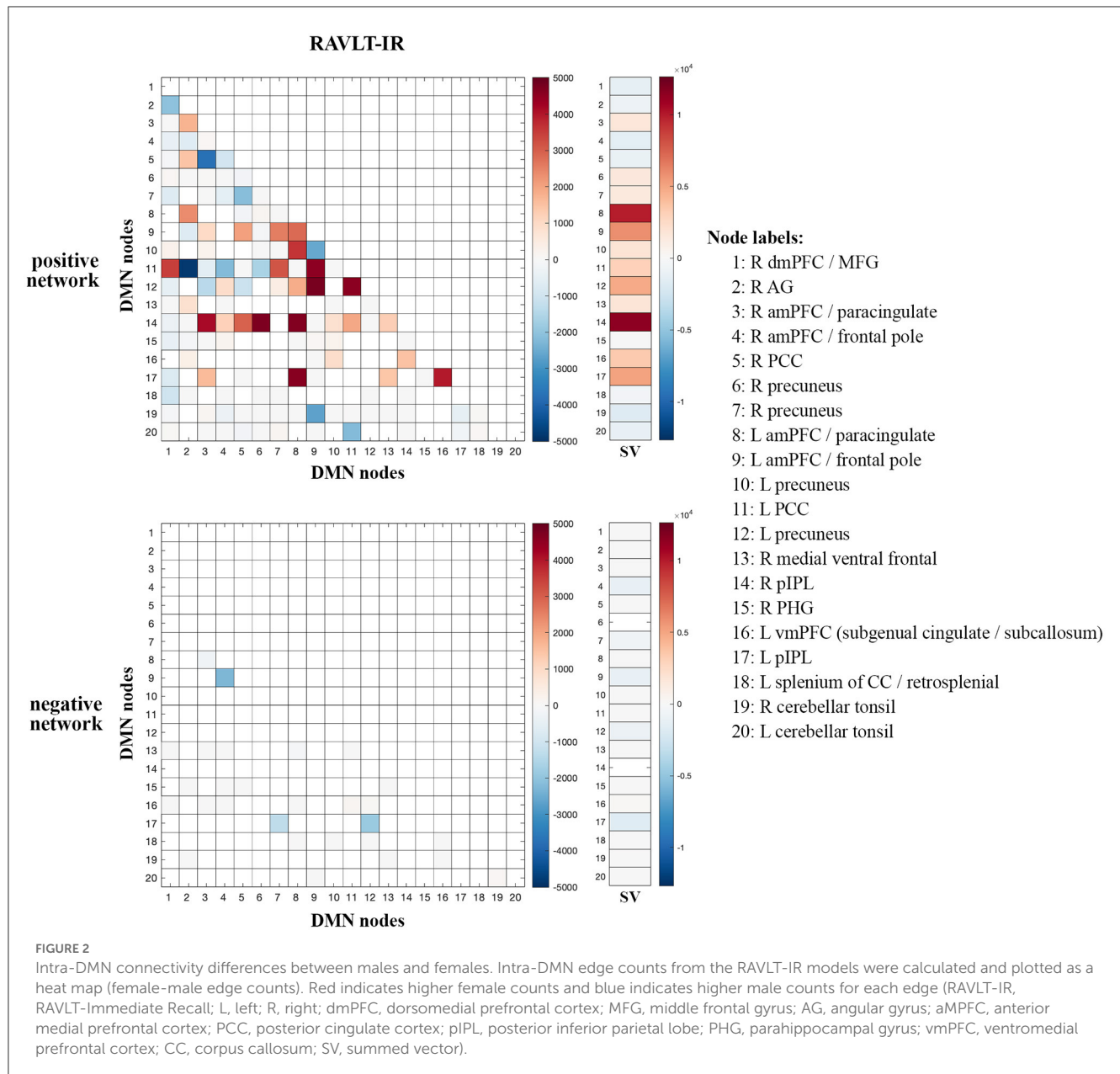


**TABLE 2 Network segregation differences between female and male subjects.**

Scan type	Default mode network (DMN)	Visual I (VI) network	Visual II (VII) network	Visual association areas (VAs)
REST1_AP	3.17 (0.0016)	-1.32 (0.1879) <sup>†</sup>	-9.02 (2.69E-18)	-4.32 (1.87E-05)
REST1_PA	3.45 (0.0006)	-0.40 (0.6920) <sup>†</sup>	-7.79 (3.18E-14)	-3.92 (0.0001)
REST2_AP	1.21 (0.2259) <sup>†</sup>	-0.92 (0.3557) <sup>†</sup>	-7.07 (4.42E-12)	-5.16 (3.47E-07)
REST2_PA	2.04 (0.0419) <sup>†</sup>	0.07 (0.9425) <sup>†</sup>	-6.38 (3.66E-10)	-2.55 (0.0111)
CART	2.57 (0.0104)	2.11 (0.0349) <sup>†</sup>	-5.33 (1.40E-07)	-0.54 (0.5864) <sup>†</sup>
FACENAME	1.18 (0.2397) <sup>†</sup>	1.74 (0.0821) <sup>†</sup>	-4.46 (9.71E-06)	-1.03 (0.3017) <sup>†</sup>
VISMOTOR	0.20 (0.8399) <sup>†</sup>	-0.47 (0.6360) <sup>†</sup>	-3.33 (0.0009)	-3.06 (0.0023)

Two-sample t-tests comparing the association ratios for networks of interest between the sexes revealed increased DMN segregation in female subjects and increased VII and VAs network segregation in male subjects. Red indicates significantly higher network segregation in female subjects than male subjects and blue indicates significantly higher network segregation in male subjects than female subjects. We report these results as “t-statistic (p-value)” in the table. <sup>†</sup> indicates the models that did not survive correction for multiple comparisons.

functional segregation over the course of aging and during memory task performance specifically (Ingallhalikar et al., 2014; Rabipour et al., 2021; Subramaniapillai et al., 2022), potentially relating to AD vulnerability (Rabipour et al., 2021). We show that sex differences in segregation are network-specific: women have relatively decreased segregation of visual sensory and visual association networks, but increased DMN segregation relative to men.

## 5. Limitations and future directions

While the HCP-A dataset has many strengths, it has limitations. Specifically, while the dataset is large and offers very high-quality neuroimaging and neuropsychological characterization, it is cross-sectional, so we cannot assess for longitudinal effects. Second, amyloid biomarkers are not available for the participants, so we cannot examine the effect of preclinical AD on the measures of interest. Third, the average education level of the participants in HCP-A is high (15.5 years), which may limit the generalizability of this model to individuals with lower access to education.

In terms of our results, we identify specific edges within the brain connectome and within the DMN in particular that contribute to memory performance in women specifically. The translational impact of these findings will depend on future work investigating whether these edges share a common gene expression pattern or other characteristic at the cellular level, which could be leveraged toward a potential therapeutic target. Additionally, our analyses suggest that edges between the visual sensory networks and the cerebellum may play an important role in memory performance, particularly for women. Future analyses that parcellate the cerebellum will be important for interpreting this finding, given that the cerebellum participates in many intrinsic connectivity networks (Buckner et al., 2011). Although CPM includes internal cross-validation, ensuring the robustness of our model, another important future direction is to test the generalizability of our model in another dataset of healthy aging. It will also be important to test whether our model can predict memory performance in individuals with preclinical and symptomatic AD, in order to assess whether it is able to predict the cognitive decline associated with symptomatic illness, in addition to predicting variance in health.

Finally, our work addresses the impact of self-reported sex on network changes, but AD risk in women also depends upon gender-based factors such as lack of access to activities which promote cognitive reserve, such as cardiovascular exercise, occupational complexity, and educational attainment (Mielke et al., 2014). Additionally, the interplay of assigned sex at birth and gender identity was not assessed due to a lack of the required information in the HCP dataset. While we used self-identified sex to distinguish subjects, this categorization may not capture the complex dynamics that may contribute to the sex differences described above. Future work should seek to incorporate other variables, as has been recently suggested regarding ovarian hormone status (Rocks et al., 2022), and to incorporate metrics of cognitive reserve.

## 6. Conclusion

In summary, this study makes three key contributions to our understanding of sex differences in brain circuitry driving memory performance, which could have implications for women's higher vulnerability to AD. First, we found that women relied more on within-network DMN edges (specifically bilateral posterior inferior parietal lobe and its connections to the major DMN hubs, medial prefrontal cortex and posterior cingulate/precuneus) for memory task performance than did men. Second, we determined that men's memory task performance was predicted by edges distributed more broadly both within and between visual sensory and visual association networks and the medial frontal network. Finally, in contrast to prior literature which suggests increased generalization of cognitive circuits in aging women, we show that women have relatively greater functional segregation of the DMN than men during memory task performance.

This work adds to the growing literature suggesting that women rely more on the DMN than do men both at rest and during memory task performance. At rest, women have relatively higher DMN connectivity (Biswal et al., 2010; Scheinost et al., 2015; Cavado et al., 2018; Ritchie et al., 2018; Ficek-Tani et al., 2022), with higher posterior DMN connectivity particularly during the menopausal decades (Ficek-Tani et al., 2022); this increased connectivity correlates with better performance on tests of short-term memory (Fredericks et al., 2019; Natu et al., 2019; Kang et al., 2021; Vanneste et al., 2021; Ficek-Tani et al., 2022). This profile is similar to individuals with preclinical (amyloid- $\beta$  +) or elevated genetic risk (e.g., APOE- $\epsilon$ 4+) for AD (Bookheimer et al., 2000; Filippini et al., 2009; Sperling et al., 2009; Mormino et al., 2011; Schultz et al., 2017).

We need to understand why AD has a more aggressive phenotype in women. Taken together this work adds to a body of literature that suggests that women's relative increased reliance on within-DMN connectivity could lead to "overuse" and vulnerability of this network to pathology over time. Future work examining the common cellular features of the nodes composing women's strongest predictive edges have the potential to translate as therapeutic targets.

## Data availability statement

The original contributions presented in the study are included in the article/Supplementary material, further inquiries can be directed to the corresponding author.

## Ethics statement

Ethical review and approval was not required for the study on human participants in accordance with the local legislation and institutional requirements. The patients/participants provided their written informed consent to participate in this study.

## Author contributions

SJ, CH, RC, and CF conceived of the presented idea. SJ and CF developed the theory and specified assessment parameters. CH, XS, and RC developed computational models. SJ, CH, HA, and AT performed computations. SJ performed visualizations of the results. RC helped supervise the project. CF supervised the project. SJ, CH, HA, AT, and CF drafted the original manuscript. All authors discussed the results and contributed to the manuscript.

## Funding

This work was funded by awards to CF from the National Institutes of Health (5K23AG059919-04), the Alzheimer's Association (2019-AACSF-644153), a Development Award from the Yale Alzheimer's Disease Research Center (P30AG0066508), Women's Health Research at Yale, and the McCance Foundation. Research reported in this publication was supported by the National Institute on Aging of the National Institutes of Health under Award Number U01AG052564 and by funds provided by the McDonnell Center for Systems Neuroscience at Washington University in St. Louis.

## Acknowledgments

We thank Bronte Ficek-Tani for her assistance in preprocessing the HCP-A fMRI data used in this study and the Human Connectome Project-Lifespan team for making the HCP-A dataset available to the research community. We also thank the National Institutes of Health (5K23AG059919-04), the Alzheimer's Association (2019-AACSF-644153), Women's Health Research

at Yale, and the McCance Foundation for their support of this work.

## Conflict of interest

The authors declare that the research was conducted in the absence of any commercial or financial relationships that could be construed as a potential conflict of interest.

## Publisher's note

All claims expressed in this article are solely those of the authors and do not necessarily represent those of their affiliated organizations, or those of the publisher, the editors and the reviewers. Any product that may be evaluated in this article, or claim that may be made by its manufacturer, is not guaranteed or endorsed by the publisher.

## Author disclaimer

The content is solely the responsibility of the authors and does not necessarily represent the official views of the National Institutes of Health.

## Supplementary material

The Supplementary Material for this article can be found online at: <https://www.frontiersin.org/articles/10.3389/frdem.2023.1126016/full#supplementary-material>

## References

- '2022 Alzheimer's disease facts and figures' (2022). *Alzheimers Dement.* 18, 700–789. doi: 10.1002/alz.12638
- Barnes, L. L., Wilson, R. S., Bienias, J. L., Schneider, J. A., Evans, D. A., and Bennett, D. A. (2005). Sex differences in the clinical manifestations of Alzheimer disease pathology. *Arch. Gen. Psychiatry.* 62, 685–691. doi: 10.1001/archpsyc.62.6.685
- Bean, J. (2011). Rey Auditory Verbal Learning Test, Rey AVLT, in *Encyclopedia of Clinical Neuropsychology*, eds J.S. Kreutzer, J. DeLuca, and B. Caplan (New York, NY: Springer), 2174–2175.
- Benjamini, Y., and Hochberg, Y. (1995). Controlling the false discovery rate: a practical and powerful approach to multiple testing. *J. R. Stat. Soc. Series B Stat. Methodol.* 57, 289–300. doi: 10.1111/j.2517-6161.1995.tb02031.x
- Biswal, B. B., Mennes, M., Zuo, X.-N., Gohel, S., Kelly, C., Smith, S. M., et al. (2010). Toward discovery science of human brain function. *Proc. Natl. Acad. Sci. U S A.* 107, 4734–4739. doi: 10.1073/pnas.0911855107
- Bleecker, M. L., Bolla-Wilson, K., Agnew, J., and Meyers, D. A. (1988). Age-related sex differences in verbal memory. *J. Clin. Psychol.* 44, 403–411.
- Bondi, M. W., Houston, W. S., Eyler, L. T., and Brown, G. G. (2005). fMRI evidence of compensatory mechanisms in older adults at genetic risk for Alzheimer disease. *Neurology.* 64, 501–508. doi: 10.1212/01.WNL.0000150885.00929.7E
- Bookheimer, S. Y., Salat, D. H., Terpstra, M., Ances, B. M., Barch, D. M., Buckner, R. L., et al. (2019). The lifespan human connectome project in aging: an overview. *NeuroImage.* 185, 335–348. doi: 10.1016/j.neuroimage.2018.10.009
- Bookheimer, S. Y., Strojwias, M. H., Cohen, M. S., Saunders, A. M., Pericak-Vance, M. A., Mazziotta, J. C., et al. (2000). Patterns of Brain Activation in People at Risk for Alzheimer's Disease. *N. Engl. J. Med.* 343, 450–456. doi: 10.1056/NEJM200008173430701
- Brewer, C. A. (2022). *ColorBrewer Brewermap Function*. Available online at: <http://colorbrewer.org/>
- Brier, M. R., Thomas, J. B., Snyder, A. Z., Benzinger, T. L., Zhang, D., Raichle, M. E., et al. (2012). Loss of intranetwork and internetwork resting state functional connections with Alzheimer's disease progression. *J. Neurosci.* 32, 8890–9. doi: 10.1523/JNEUROSCI.5698-11.2012
- Buckley, R. F., Mormino, E. C., Amariglio, R. E., Properzi, M. J., Rabin, J. S., Lim, Y. Y., et al. (2018). Sex, amyloid, and APOE ε4 and risk of cognitive decline in preclinical Alzheimer's disease: Findings from three well-characterized cohorts. *Alzheimer's Dement.* 14, 1193–1203. doi: 10.1016/j.jalz.2018.04.010
- Buckner, R. L., Krienen, F. M., Castellanos, A., Diaz, J. C., and Yeo, B. T. T. (2011). The organization of the human cerebellum estimated by intrinsic functional connectivity. *J. Neurophysiol.* 106, 2322–2345. doi: 10.1152/jn.00339.2011
- Cassady, K. E., Adams, J. N., Chen, X., Maass, A., Harrison, T. M., Landau, S., et al. (2021). Alzheimer's pathology is associated with dedifferentiation of intrinsic functional memory networks in aging. *Cereb. Cortex.* 31, 4781–4793. doi: 10.1093/cercor/bhab122
- Cavedo, E., Chiesa, P. A., Houot, M., Ferretti, M. T., Grothe, M. J., Teipel, S. J., et al. (2018). Sex differences in functional and molecular neuroimaging biomarkers of Alzheimer's disease in cognitively normal older adults with subjective memory complaints. *Alzheimer's Dement.* 14, 1204–1215. doi: 10.1016/j.jalz.2018.05.014

- Chan, M. Y., Park, D. C., Savalia, N. K., Petersen, S. E., and Wig, G. S. (2014). Decreased segregation of brain systems across the healthy adult lifespan. *Proc. Natl. Acad. Sci. U S A*. 111, E4997–E5006. doi: 10.1073/pnas.1415122111
- Costa, P. T. Jr., and McCrae, R. R. (1992). *Revised NEO Personality Inventory (NEO-PI-R) and NEO Five-Factor Inventory (NEO-FFI) professional manual*. Odessa, FL.
- Dufford, A. J., Kimble, V., Tejavibulya, L., Dadashkarimi, J., and Scheinost, D. (2023). Predicting Transdiagnostic Social Impairments in Childhood using Connectome-based Predictive Modeling. *Psychiatry Clin. Psychol.* 91, S87. doi: 10.1016/j.biopsycho.2022.02.234
- Edwards, L., Joie, R. L., Iaccarino, L., Strom, A., Baker, S. L., Casaletto, K. B., et al. (2021). Multimodal neuroimaging of sex differences in cognitively impaired patients on the Alzheimer's continuum: greater tau-PET retention in females. *Neurobiol. Aging*. 105, 86–98. doi: 10.1016/j.neurobiolaging.2021.04.003
- Estévez-González, A., Kulisevsky, J., Boltes, A., Otermín, P., and García-Sánchez, C. (2023). Rey verbal learning test is a useful tool for differential diagnosis in the preclinical phase of Alzheimer's disease: comparison with mild cognitive impairment and normal aging. *Int. J. Geriatr. Psychiatry*. 18, 1021–1028. doi: 10.1002/gps.1010
- Ferretti, M. T., Iulita, M. F., Cavedo, E., Chiesa, P. A., Dimech, A. S., Chadha, A. S., et al. (2018). Sex differences in Alzheimer disease — the gateway to precision medicine. *Nat. Rev. Neurol.* 14, 457–469. doi: 10.1038/s41582-018-0032-9
- Fickel-Tani, B., Horien, C., Ju, S., Xu, W., Li, N., Lacadie, C., et al. (2022). Sex differences in default mode network connectivity in healthy aging adults. *Cereb. Cortex*. bhac491. doi: 10.1093/cercor/bhac491. [Epub ahead of print].
- Filippini, N., MacIntosh, B. J., Hough, M. G., Goodwin, G. M., Frisoni, G. B., Smith, S. M., et al. (2009). Distinct patterns of brain activity in young carriers of the APOE-ε4 allele. *Proc. Natl. Acad. Sci. U.S.A.* 106, 7209–7214. doi: 10.1073/pnas.0811879106
- Fredericks, C. A., Brown, J. A., Deng, J., Kramer, A., Ossenkoppele, R., Rankin, K., et al. (2019). Intrinsic connectivity networks in posterior cortical atrophy: a role for the pulvinar?. *Neuroimage Clin.* 21, 101628. doi: 10.1016/j.nicl.2018.101628
- Gabrieli, J. D. E., Ghosh, S. S., and Whitfield-Gabrieli, S. (2015). Prediction as a humanitarian and pragmatic contribution from human cognitive neuroscience. *Neuron*. 85, 11–26. doi: 10.1016/j.neuron.2014.10.047
- Geerligs, L., Renken, R. J., Saliassi, E., Maurits, N. M., and Lorist, M. M. (2015). A brain-wide study of age-related changes in functional connectivity. *Cereb. Cortex*. 25, 1987–1999. doi: 10.1093/cercor/bhu012
- Golchert, J., Roehrer, S., Luck, T., Wagner, M., Fuchs, A., Wiese, B., et al. (2019). Women outperform men in verbal episodic memory even in oldest-old age: 13-year longitudinal results of the AgeCoDe/AgeQualiDe Study. *J. Alzheimer's Dis.* 69, 857–869. doi: 10.3233/JAD-180949
- Greene, A. S., Gao, S., Scheinost, D., and Constable, R. T. (2018). Task-induced brain state manipulation improves prediction of individual traits. *Nat. Commun.* 9, 1–13. doi: 10.1038/s41467-018-04920-3
- Greicius, M. D., Srivastava, G., Reiss, A. L., and Menon, V. (2004). Default-mode network activity distinguishes Alzheimer's disease from healthy aging: evidence from functional MRI. *Proc. Natl. Acad. Sci. U S A*. 101, 4637–42. doi: 10.1073/pnas.0308627101
- Harms, M. P., Somerville, L. H., Ances, B. M., Andersson, J., Barch, D. M., Bastiani, M., et al. (2018). Extending the human connectome project across ages: imaging protocols for the lifespan development and aging projects. *NeuroImage*. 183, 972–984. doi: 10.1016/j.neuroimage.2018.09.060
- Herlitz, A., Nilsson, L. G., and Bäckman, L. (1997). Gender differences in episodic memory. *Mem. Cognit.* 25, 801–811. doi: 10.3758/BF03211324
- Horien, C., Greene, A. S., Shen, X., Fortes, D., Brennan-Wydra, E., Banarjee, C., et al. (2022). A generalizable connectome-based marker of in-scan sustained attention in neurodiverse youth. *Cereb. Cortex*. bhac506. doi: 10.1093/cercor/bhac506. [Epub ahead of print].
- Horien, C., Noble, S., Finn, E. S., Shen, X., Scheinost, D., and Constable, R. T. (2018). Considering factors affecting the connectome-based identification process: Comment on Waller et al. *NeuroImage*. 169, 172–175. doi: 10.1016/j.neuroimage.2017.12.045
- Horien, C., Shen, X., Scheinost, D., and Constable, R. T. (2019). The individual functional connectome is unique and stable over months to years. *NeuroImage*. 189, 676–687. doi: 10.1016/j.neuroimage.2019.02.002
- Ingalhalikar, M., Smith, A., Parker, D., Satterthwaite, T. D., Elliott, M. A., Ruparel, K., et al. (2014). Sex differences in the structural connectome of the human brain. *Proc. Natl. Acad. Sci. U.S.A.* 111, 823–828. doi: 10.1073/pnas.1316909110
- Joshi, A., Scheinost, D., Okuda, H., Belhachemi, D., Murphy, I., Staib, L. H., et al. (2011). Unified framework for development, deployment and robust testing of neuroimaging algorithms. *Neuroinformatics*. 9, 69–84. doi: 10.1007/s12021-010-9092-8
- Ju, Y., Horien, C., Chen, W., Guo, W., Lu, X., Sun, J., et al. (2020). Connectome-based models can predict early symptom improvement in major depressive disorder. *J. Affect. Disord.* 273, 442–452. doi: 10.1016/j.jad.2020.04.028
- Kang, D. W., Wang, S.-M., Um, Y. H., Na, H.-R., Kim, N.-Y., Lee, C. U., et al. (2021). Distinctive association of the functional connectivity of the posterior cingulate cortex on memory performances in early and late amnesic mild cognitive impairment patients. *Front. Aging Neurosci.* 13, 696735. doi: 10.3389/fnagi.2021.696735
- Lutkenhoff, E. S., Rosenberg, M., Chiang, J., Zhang, K., Pickard, J. D., Owen, A. M., et al. (2014). Optimized brain extraction for pathological brains (optiBET). *PLoS ONE*. 9, e115551. doi: 10.1371/journal.pone.0115551
- Marek, S., Tervo-Clemmens, B., Calabro, F. J., Montez, D. F., Kay, B. P., Hatoun, A. S., et al. (2022). Reproducible brain-wide association studies require thousands of individuals. *Nature*. 603, 654–660. doi: 10.1038/s41586-022-04492-9
- Mielke, M. M., Vemuri, P., and Rocca, W. A. (2014). Clinical epidemiology of Alzheimer's disease: assessing sex and gender differences. *Clin. Epidemiol.* 6, 37–48. doi: 10.2147/CLEP.S37929
- Moradi, E., Hallikainen, I., Hänninen, T., Tohka, J., and Initiative, A. D. N. (2017). Rey's auditory verbal learning test scores can be predicted from whole brain MRI in Alzheimer's disease. *Neuroimage Clin.* 13, 415–427. doi: 10.1016/j.nicl.2016.12.011
- Mormino, E. C., Smiljic, A., Hayenga, A. O., Onami, S. H., Greicius, M. D., Rabinovici, G. D., et al. (2011). Relationships between beta-amyloid and functional connectivity in different components of the default mode network in aging. *Cereb. Cortex*. 21, 2399–407. doi: 10.1093/cercor/bhr025
- Nasreddine, Z. S., Phillips, N. A., Bédirian, V., Charbonneau, S., Whitehead, V., Collin, I., et al. (2005). The montreal cognitive assessment, MoCA: a brief screening tool for mild cognitive impairment. *J. Am. Geriatr. Soc.* 53, 695–699. doi: 10.1111/j.1532-5415.2005.53221.x
- Natu, V. S., Lin, J.-J., Burks, A., Arora, A., Rugg, M. D., and Lega, B. (2019). Stimulation of the posterior cingulate cortex impairs episodic memory encoding. *J. Neurosci.* 39, 7173–7182. doi: 10.1523/JNEUROSCI.0698-19.2019
- Ng, K. K., Lo, J. C., Lim, J. K. W., Chee, M. W. L., and Zhou, J. (2016). Reduced network segregation between the default mode network and the executive control network in healthy older adults: a longitudinal study. *NeuroImage*. 133, 321–330. doi: 10.1016/j.neuroimage.2016.03.029
- Pearce, J. W. (2007). PsychoPy—Psychophysics software in Python. *J. Neurosci. Methods*. 162, 8–13. doi: 10.1016/j.jneumeth.2006.11.017
- Pearce, J. W. (2008). Generating stimuli for neuroscience using PsychoPy. *Front. Neuroinform.* 2, 10. doi: 10.3389/neuro.11.010.2008
- Poldrack, R. A., Huckins, G., and Varoquaux, G. (2020). Establishment of best practices for evidence for prediction: a review. *JAMA psychiatry*. 77, 534–540. doi: 10.1001/jamapsychiatry.2019.3671
- Qi, Z., Wu, X., Wang, Z., Zhang, N., Dong, H., Yao, L., et al. (2010). Impairment and compensation coexist in amnesic MCI default mode network. *NeuroImage*. 50, 48–55. doi: 10.1016/j.neuroimage.2009.12.025
- Rabipour, S., Rajagopal, S., Pasvanis, S., Group, P.-A. R., and Rajah, M. N. (2021). Generalization of memory-related brain function in asymptomatic older women with a family history of late onset Alzheimer's disease: results from the PREVENT-AD cohort. *Neurobiol. Aging*. 104, 42–56. doi: 10.1016/j.neurobiolaging.2021.03.009
- Ritchie, S. J., Cox, S. R., Shen, X., Lombardo, M. V., Reus, L. M., Alloza, C., et al. (2018). Sex differences in the adult human brain: evidence from 5216 UK biobank participants. *Cereb. Cortex*. 28, 2959–2975. doi: 10.1093/cercor/bhy109
- Rocks, D., Cham, H., and Kundakovic, M. (2022). Why the estrous cycle matters for neuroscience. *Biol. Sex Differ.* 13, 62. doi: 10.1186/s13293-022-00466-8
- Rosenberg, M. D., Casey, B. J., and Holmes, A. J. (2018). Prediction complements explanation in understanding the developing brain. *Nature Commun.* 9, 589. doi: 10.1038/s41467-018-02887-9
- Rosenberg, M. D., Finn, E. S., Scheinost, D., Papademetris, X., Shen, X., Constable, R. T., et al. (2016). A neuromarker of sustained attention from whole-brain functional connectivity. *Nature Neurosci.* 19, 165–171. doi: 10.1038/nn.4179
- Satterthwaite, T. D., Elliott, M. A., Gerraty, R. T., Ruparel, K., Loughead, J., Calkins, M. E., et al. (2013). An improved framework for confound regression and filtering for control of motion artifact in the preprocessing of resting-state functional connectivity data. *Neuroimage*. 64, 240–256. doi: 10.1016/j.neuroimage.2012.08.052
- Scheinost, D., Dadashkarimi, J., Finn, E. S., Wambach, C. G., MacGillivray, C., Roule, A. L., et al. (2021). Functional connectivity during frustration: a preliminary study of predictive modeling of irritability in youth. *Neuropsychopharmacology*. 46, 1300–1306. doi: 10.1038/s41386-020-00954-8
- Scheinost, D., Finn, E. S., Tokoglu, F., Shen, X., Papademetris, X., Hampson, M., et al. (2015). Sex differences in normal age trajectories of functional brain networks. *Hum. Brain Mapp.* 36, 1524–1535. doi: 10.1002/hbm.22720
- Scheinost, D., Noble, S., Horien, C., Greene, A. S., Lake, E. M., Salehi, M., et al. (2019). Ten simple rules for predictive modeling of individual differences in neuroimaging. *NeuroImage*. 193, 35–45. doi: 10.1016/j.neuroimage.2019.02.057
- Schultz, A. P., Chhatwal, J. P., Hedden, T., Mormino, E. C., Hanseeuw, B. J., Sepulcre, J., et al. (2017). Phases of hyperconnectivity and hypoconnectivity in the default mode and salience networks track with amyloid and tau in clinically normal individuals. *J. Neurosci.* 37, 4323–4331. doi: 10.1523/JNEUROSCI.3263-16.2017
- Sheline, Y. I., Raichle, M. E., Snyder, A. Z., Morris, J. C., Head, D., Wang, S., et al. (2010). Amyloid plaques disrupt resting state default mode network connectivity in cognitively normal elderly. *Biol. Psychiatry*, 67, 584–7. doi: 10.1016/j.biopsycho.2009.08.024

- Shen, X., Finn, E. S., Scheinost, D., Rosenberg, M. D., Chun, M. M., Papademetris, X., et al. (2017). Using connectome-based predictive modeling to predict individual behavior from brain connectivity. *Nat. Protoc.* 12, 506–518. doi: 10.1038/nprot.2016.178
- Shen, X., Tokoglu, F., Papademetris, X., and Constable, R. T. (2013). Groupwise whole-brain parcellation from resting-state fMRI data for network node identification. *NeuroImage*. 82, 403–415. doi: 10.1016/j.neuroimage.2013.05.081
- Sperling, R. A., Laviolette, P. S., O'Keefe, K., O'Brien, J., Rentz, D. M., Pihlajamaki, M., et al. (2009). Amyloid deposition is associated with impaired default network function in older persons without dementia. *Neuron*. 63, 178–188. doi: 10.1016/j.neuron.2009.07.003
- Subramaniapillai, S., Rajagopal, S., Ankudowich, E., Pasvanis, S., Mistic, B., and Rajah, M. N. (2022). Age- and episodic memory-related differences in task-based functional connectivity in women and men. *J. Cogn. Neurosci.* 34, 1500–1520. doi: 10.1162/jocn\_a\_01868
- Vanneste, S., Luckey, A., McLeod, S. L., Robertson, I. H., and To, W. T. (2021). Impaired posterior cingulate cortex–parahippocampus connectivity is associated with episodic memory retrieval problems in amnesic mild cognitive impairment. *Eur. J. Neurosci.* 53, 3125–3141. doi: 10.1111/ejn.15189
- Yarkoni, T. (2022). The generalizability crisis. *Behav. Brain Sci.* 45, e1. doi: 10.1017/S0140525X21001758
- Yarkoni, T., and Westfall, J. (2017). Choosing prediction over explanation in psychology: lessons from machine learning. *Perspect Psychol. Sci.* 12, 1100–1122. doi: 10.1177/1745691617693393
- Yip, S. W., Scheinost, D., Potenza, M. N., and Carroll, K. M. (2019). Connectome-based prediction of cocaine abstinence. *Am. J. Psychiatry.* 176, 156–164. doi: 10.1176/appi.ajp.2018.17101147